

## ORIGINAL ARTICLE

Translocations at 8q24 juxtapose *MYC* with genes that harbor superenhancers resulting in overexpression and poor prognosis in myeloma patientsBA Walker<sup>1</sup>, CP Wardell<sup>1</sup>, A Brioli<sup>1,2</sup>, E Boyle<sup>1</sup>, MF Kaiser<sup>1</sup>, DB Begum<sup>1</sup>, NB Dahir<sup>1</sup>, DC Johnson<sup>1</sup>, FM Ross<sup>3</sup>, FE Davies<sup>4</sup> and GJ Morgan<sup>1</sup>

Secondary *MYC* translocations in myeloma have been shown to be important in the pathogenesis and progression of disease. Here, we have used a DNA capture and massively parallel sequencing approach to identify the partner chromosomes in 104 presentation myeloma samples. 8q24 breakpoints were identified in 21 (20%) samples with partner loci including *IGH*, *IGK* and *IgL*, which juxtapose the immunoglobulin (Ig) enhancers next to *MYC* in 8/23 samples. The remaining samples had partner loci including *XBPI*, *FAM46C*, *CCND1* and *KRAS*, which are important in B-cell maturation or myeloma pathogenesis. Analysis of the region surrounding the breakpoints indicated the presence of superenhancers on the partner chromosomes and gene expression analysis showed increased expression of *MYC* in these samples. Patients with *MYC* translocations had a decreased progression-free and overall survival. We postulate that translocation breakpoints near *MYC* result in colocalization of the gene with superenhancers from loci, which are important in the development of the cell type in which they occur. In the case of myeloma these are the Ig loci and those important for plasma cell development and myeloma pathogenesis, resulting in increased expression of *MYC* and an aggressive disease phenotype.

*Blood Cancer Journal* (2014) 4, e191; doi:10.1038/bcj.2014.13; published online 14 March 2014

## INTRODUCTION

Rearrangements at 8q24 have been reported in up to 47% of myeloma patients by a combination of fluorescence *in situ* hybridization (FISH), spectral karyotyping and classical cytogenetics.<sup>1</sup> In presenting myeloma this frequency is lower, with abnormalities of 8q reported in 15% of cases using mapping arrays and FISH.<sup>2,3</sup> The gene of interest in this region is *MYC*, an oncogene that has a pivotal role in cell growth, proliferation, tumorigenesis and stem cells.<sup>4</sup>

The importance of *MYC* activation in myeloma has been shown through the use of the *Vk\*MYC* transgenic mouse model, where activation of *MYC* arises through AID-dependent somatic hypermutation during B-cell development, resulting in the onset of myeloma in these mice.<sup>5</sup> *MYC* has also been shown to be activated in the transition from monoclonal gammopathy of undetermined significance to myeloma, implicating it in disease progression.<sup>6</sup> Myeloma cells have been shown to have a dependency on *MYC* for survival, where inhibition of *MYC* by small hairpin RNA or small-molecule inhibitors results in cell death indicating that *MYC* is a promising therapeutic target.<sup>7</sup>

The mechanism of *MYC* activation is mainly through secondary translocations involving the immunoglobulin (Ig) loci (*IGH* > *IgL* > *IGK*), which juxtapose the strong B-cell enhancers present at these loci and *MYC*, resulting in overexpression of the oncogene.<sup>8</sup> Unlike primary translocations in myeloma, which are often simple reciprocal exchanges of chromosomal material, the rearrangements that result from *MYC* translocations are often complex, involving many partner chromosomes.<sup>1,8</sup> Interestingly, it has been reported that up to 74% of *MYC* rearrangements do not involve an Ig locus<sup>3</sup> leading to the conclusion that other

mechanisms of activation may also be important in myeloma. Using FISH, partner chromosomes at 1p13, 1p21–22, 6p21, 6q12–15, 13q14 and 16q22 have been identified, but the specific loci involved have remained elusive.<sup>3,9–11</sup>

The breakpoints on 8q24 have been mapped in a large number of myeloma cell lines and the majority are found within 1 Mb of *MYC*, but some can be greater than 3 Mb either telomeric or centromeric of the locus.<sup>8,12,13</sup> The loci surrounding *MYC* are *POU5F1B* (centromeric) and *PVT1* (telomeric). *PVT1* is a non-coding RNA that has been shown to be the location of variant t(8;22) breakpoints in Burkitt's lymphoma,<sup>14</sup> as well as generating fusion genes with *WVVOX* and *NBEA* in myeloma patients with an 8q24 rearrangement.<sup>13</sup>

Here, we have used targeted capture followed by massively parallel sequencing to pull down the region surrounding *MYC* in a series of presenting myeloma cases in order to identify any translocations in this area and the mechanism of action involved.

## MATERIALS AND METHODS

## Cell selection

CD138-positive bone marrow plasma cells were selected to a purity >95% using magnetic assisted cell sorting (Miltenyi Biotech, Biscy, UK). Tumor DNA and RNA were extracted using the AllPrep kit (Qiagen, Manchester, UK). All patients were at presentation and had not received any treatment when the sample was taken.

## FISH

Probes have been previously published with the addition of the *LPL* (8p22), CEP 8 and *MYC* (8q24.1–24.21) probes (Abbott, Maidenhead, UK).<sup>15–17</sup>

<sup>1</sup>Division of Molecular Pathology, The Institute of Cancer Research, London, UK; <sup>2</sup>Istituto di Ematologia Seragnoli, Università degli Studi di Bologna, Policlinico S. Orsola-Malpighi, Bologna, Italy; <sup>3</sup>Wessex Regional Genetics Laboratory, Salisbury District Hospital, Salisbury, UK and <sup>4</sup>Divisions of Molecular Pathology, Cancer Therapeutics and Clinical Sciences, The Institute of Cancer Research, London, UK. Correspondence: Professor G Morgan, Division of Molecular Pathology, The Institute of Cancer Research, London SM2 5NG, Surrey, UK.

E-mail: gareth.morgan@icr.ac.uk

Received 30 January 2014; accepted 6 February 2014

MYC abnormalities were defined using the t(8;14) fusion probe, *LPL/CEP 8/MYC* probes, *IGH@* translocations (*IGH@* break-apart probe followed by fusion probes for the common partner chromosomes). FISH results were interpreted alongside karyotype data, where available.

### Targeted capture of the *MYC* locus

A targeted capture system was designed using the SureSelect system (Agilent, Santa Clara, CA, USA) that was based on tiling RNA baits across the *MYC*, *IGH*, *IGK* and *IGL* loci as previously described.<sup>18</sup> The region captured surrounding *MYC* spanned from 127.5–129.8 Mb on chromosome 8, roughly 1 Mb on either side of *MYC*, which is located at 128.75 Mb. This region includes *POU5F1B* and *PVT1*, which are common sites of 8q24 translocations in myeloma.

DNA from 104 samples were assayed using 150 ng of DNA and a modified capture protocol with eight cycles of prehybridization PCR and 11 cycles of posthybridization PCR. Samples were barcoded using Illumina (San Diego, CA, USA) indexes and up to 27 samples were sequenced per lane on a HiSeq2000 generating 76-bp paired-end reads. After base calling and quality control metrics, the raw fastq reads were aligned to the reference human genome (build GRCh37) resulting in a median depth of 289 × per sample after de-duplication for the captured region.

Translocation breakpoints were identified in the sequencing data using DELLY.<sup>19</sup> Breakpoints called using the bioinformatic approach were further filtered based on depth, unique mappability for 76bp reads, number of supporting reads and whether or not they were detected in non-tumor samples. The coordinates of the breakpoints and superenhancers were compared with randomized data produced using Monte Carlo sampling using the Genomic Hyper Browser.<sup>20</sup>

Statistical analyses were performed using SPSS version 19.0 (SPSS Inc., Chicago, IL, USA). Discrete data were expressed as frequencies and percentages and were assessed by Fisher's exact test or the  $\chi^2$ -test, as appropriate. Survival curves were plotted using the Kaplan–Meier method. Differences between curves were tested for statistical significance using the log-rank test. A multivariate Cox regression analysis was done to identify factors significantly associated with progression-free survival (PFS) and overall survival (OS), with statistical significance set at  $P < 0.05$ .

## RESULTS

### *MYC* rearrangements detected by FISH

*MYC* rearrangements were tested for using interphase FISH on CD138<sup>+</sup> selected plasma cells on patient samples from the UK MRC Myeloma IX trial using a combination of probes for *MYC* (8q24), *LPL* (8p22) and *CEP 8*. Interphase FISH was successful on 751 patients and was interpreted with data from FISH probes for the *IGH* locus and karyotyping. Table 1 shows the frequency of *MYC* abnormalities, split by translocation group in these samples. *MYC* abnormalities were detected in 26% of samples with the most frequent abnormality being gain of the locus, followed by a split probe signal. In 50% (32/63) of those with a split probe signal the *IGH/K/L* locus was identified as the partner. Of the 32 samples with an Ig partner 28 were with the *IGH* locus. In the remaining 50% the partner remained undetermined, but may involve the light chain loci in samples where cytogenetics or karyotyping was unsuccessful or uninformative. *MYC* rearrangements were not

associated with any particular primary translocation, but were associated with ISS II ( $P = 0.022$ ) or ISS III ( $P = 0.0027$ ). There was no negative impact on PFS or OS in patients with a *MYC* abnormality.

### *MYC* rearrangements detected by sequence capture

The presence of unidentified *MYC* partner chromosomes led us to investigate possible partner chromosomes using an alternative technique. We had previously used a DNA capture technique followed by massively parallel sequencing to identify the translocation partner chromosomes to the *IGH/K/L* loci.<sup>18</sup> In this assay we had also captured a region surrounding *MYC* and set out to identify potential partner chromosomes. A region of ~2 Mb was tiled around the *MYC* locus using RNA baits and used to capture DNA and associated translocations in this region.

We assayed 104 presentation myeloma samples for the presence of *MYC* translocations using the capture assay followed by massively parallel sequencing. The samples consisted of 55 samples from the Myeloma IX trial and an additional 49 samples from the UK Myeloma XI trial, for which FISH results are not available. The samples were categorized according to *IGH* translocation using a combination of FISH,<sup>15,21</sup> gene expression<sup>22</sup> and targeted capture of the *IGH* locus<sup>18</sup> and consisted of a variety of samples with *IGH* translocations and 8q24 rearrangements as shown in Table 2; Supplementary Table 1. Only three samples analyzed by the capture technique had a split *MYC* locus, as determined by FISH or karyotyping. In these samples the translocation was detected using the capture and was found to be the *IGH* locus in one sample (673; verifying the FISH result) and in the other two samples (29 and 1310) was found to be chromosome 6 (also seen by karyotyping in one sample).

Breakpoints were identified and mapped in 21 samples and are shown in Figure 1. We identified breakpoints in 10 samples where either FISH or karyotyping failed to identify a translocation, as well as three samples where FISH did identify a translocation and also eight samples for which no FISH data were available. Interestingly,

**Table 2.** Incidence of 8q24 breakpoints in sequence-capture samples

Translocation	Assayed (%)	With 8q24 breakpoint (% of group)	P-value
t(4;14)	13(12.5)	0(0)	0.031
t(6;14)	8(7.7)	1(12.5)	NS
t(11;14)	28(26.9)	5(17.8)	NS
t(14;16)	17(16.3)	11(64.7)	<0.001
t(14;20)	6(5.8)	1(16.6)	NS
HRD	31(29.8)	3(9.6)	0.037
Other <sup>a</sup>	1(0.9)	1(100)	NS
Total	104	21	

Abbreviations: HRD, hyperdiploidy; NS, not significant. <sup>a</sup>This sample has a secondary t(7;14).

**Table 1.** Frequency of 8q24 abnormalities detected by FISH

8q Status	Translocation (Tx) group							
	t(4;14)	t(11;14)	t(6;14)	t(14;16)	t(14;20)	HRD	HRD + Tx	None
Normal	49	74	4	17	6	294	20	90
Gain	7	17	2	8	4	46	10	17
Split	3	10	0	2	2	40	1	5
Del	5	0	0	0	0	4	1	14
Total abnormal (%)	23.4	26.7	33.3	37.0	50.0	23.2	37.5	28.5

Abbreviation: FISH, fluorescence *in situ* hybridization.

there was an enrichment for t(14;16) and a depletion of t(4;14) and hyperdiploidy associated with an 8q24 breakpoint, Table 2, which was not seen with FISH alone.

The positions of the breakpoints on 8q24 were spread out over 1.2 Mb. The majority of the breaks were situated telomeric of *PVT1* (51.5%) with 12% within *PVT1*, 15% between *MYC* and *PVT1* and 15% between *POU5F1B* and *MYC*. Of the three samples with breakpoints within *PVT1* two were found to have potential fusion genes, one with *FOXO3* and the other with *LINC00309*.

Nine samples had two breakpoints on 8q24, often with two different chromosome partners. In samples with two breakpoints, the sequencing reads indicate that *MYC* is only involved in one of the breakpoints (that is, only one side of the translocation was captured). The reason for this is not clear and will require long reads to clarify the final genomic rearrangements. Several samples had complex rearrangements resulting in multiple chromosomal

segments being joined together, often involving *MYC*, an Ig enhancer and the primary Ig partner oncogene (for example, sample 11/625 that has a t(6;14) and a t(6;8) or sample 12/0404 that has a t(11;14) and a t(8;11)). Details of breakpoints are shown in Table 3. It is possible that the Ig enhancer is influencing both the target oncogene of the primary translocation (for example, *CCND1* or *CCND3*) and *MYC* through the assembly of a complex t(8;11;14) or t(6;8;14) derivative chromosome.

Superenhancer colocalization with *MYC*

A total of 8/21 samples (38%) with *MYC* abnormalities had rearrangements with an Ig locus on the partner chromosome. Ig partner loci are recognized to upregulate expression of the target oncogene and have been shown to have clinical relevance as prognostic markers. Given that the mechanism of upregulation of

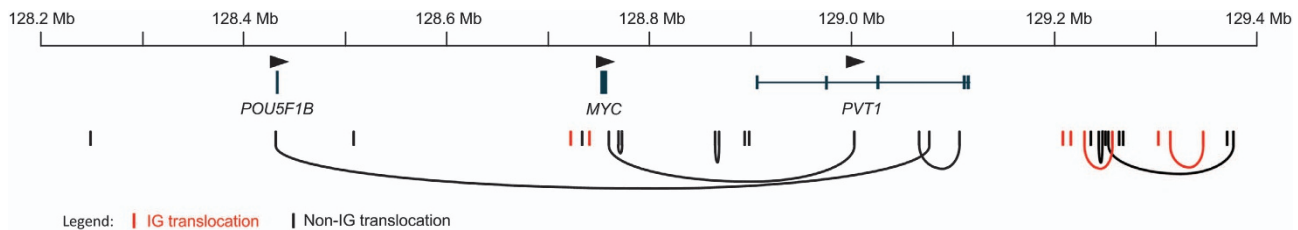


**Figure 1.** *MYC* locus breakpoints in myeloma. The locations of breakpoints are indicated by vertical lines corresponding in color to whether the partner chromosome belongs to an Ig loci (IGH@, IGK@ or IGL@; red) or a non-Ig locus (black). The genes and orientation are indicated according to their genomic location on chromosome 8. Arcs indicate the positions of two breakpoints found in one sample.

**Table 3.** Genomic locations of *MYC* breakpoints

Sample	IGH translocation	1st Chr	1st breakpoint	Part of 1st chr positioned next to chromosome 8	1st Gene <sup>a</sup>	Distance (bp) to MM1.s enhancer from breakpoint	Distance (bp) to MM1.s superenhancer from breakpoint	2 <sup>nd</sup> Chr	2 <sup>nd</sup> breakpoint	2 <sup>nd</sup> Gene <sup>a</sup>
29	t(7;14)	chr22	36779252	Telomeric	<i>MYH9</i>	0	0	chr8	129251475	<i>PVT1-CCDC26</i>
29	t(7;14)	chr6	7986298	Telomeric	<i>TXNDC5</i>	8862	8862	chr8	129375213	<i>PVT1-CCDC26</i>
176	None	chr1	118246012	Telomeric	<i>FAM46C-GDAP2</i>	16232	16232	chr8	129264632	<i>PVT1-CCDC26</i>
222	t(14;16)	chr2	64412927	Centromeric	<i>LINC00309</i>	3194	450109	chr8	129064694	<i>PVT1</i>
222	t(14;16)	chr2	64468628	Telomeric	<i>LINC00309-LGALS1</i>	12603	169177716	chr8	129104714	<i>PVT1</i>
471	None	chr22	23071965	Telomeric	<i>IGL</i>	5005	5005	chr8	128737937	<i>POU5F1B-MYC</i>
475	t(14;16)	chr12	25507375	Telomeric	<i>KRAS-IFLTD1</i>	20015	18435462	chr8	129368991	<i>PVT1-CCDC26</i>
478	t(11;14)	chr2	77937177	Telomeric	<i>LRRTM4-SNAR-H</i>	2872963	13042429	chr8	128896717 <sup>b</sup>	<i>MYC-PVT1</i>
592	t(14;16)	chr11	111195351	Telomeric	<i>C11ORF93-MIR4491</i>	36912	36912	chr8	129247671	<i>PVT1-CCDC26</i>
592	t(14;16)	chr10	122670424	Centromeric	<i>MIR5694</i>	1102347	10042441	chr8	129248430	<i>PVT1-CCDC26</i>
673	t(14;16)	chr14 <sup>c</sup>	106119946	Telomeric	<i>IGH</i>	26346	26346	chr8	129209665	<i>PVT1-CCDC26</i>
730	None	chr22	41824373	Centromeric	<i>TEF-TOB2</i>	13346	3109392	chr8	129312555	<i>PVT1-CCDC26</i>
730	None	chr22	23280899	Centromeric	<i>IGL</i>	0	0	chr8	129345574	<i>PVT1-CCDC26</i>
984	t(14;16)	chr2	89151255	Centromeric	<i>IGKC</i>	95671	2922643	chr8	129228289	<i>PVT1-CCDC26</i>
984	t(14;16)	chr2	89130434	Centromeric	<i>IGKC</i>	34641	8060442	chr8	129254453	<i>PVT1-CCDC26</i>
1112	t(11;14)	chr11	69283791	Centromeric	<i>CCND1</i>	131027	2226257	chr8	128427581	<i>POU5F1B-MYC</i>
1112	t(11;14)	chrX	146700223	Centromeric	<i>MIR510-FMR1-AS1</i>	NA <sup>d</sup>	NA <sup>d</sup>	chr8	129075004	<i>PVT1</i>
1310	t(14;16)	chr6 <sup>e</sup>	108911604	Telomeric	<i>FOXO3</i>	0	0	chr8	128761005	<i>MYC-PVT1</i>
1310	t(14;16)	chr6 <sup>e</sup>	108908007	Centromeric	<i>FOXO3</i>	0	0	chr8	129000293	<i>PVT1</i>
11/088	t(14;16)	chr10	125858805	Telomeric	<i>CHST15-OAT</i>	0	0	chr8	129235977	<i>PVT1-CCDC26</i>
11/388	t(14;16)	chr22	23307780	Centromeric	<i>IGL</i>	5757	5757	chr8	128712616	<i>POU5F1B-MYC</i>
11/625	t(6;14)	chr6	41858885	Centromeric	<i>USP49 (near CCND3)</i>	377392	10585809	chr8	128244760	<i>PCAT1-POU5F1B</i>
11/741	t(14;16)	chr22	29210349	Telomeric	<i>XBP1-ZNRF3</i>	0	0	chr8	128772206	<i>MYC-PVT1</i>
11/741	t(14;16)	chr2	134989574	Centromeric	<i>MIR3679-MGAT5</i>	47048	22523506	chr8	128772558	<i>MYC-PVT1</i>
214	t(14;20)	chr22	23285257	Centromeric	<i>IGL</i>	0	0	chr8	129214819	<i>PVT1-CCDC26</i>
11/1212	t(14;16)	chr22	23258401	Centromeric	<i>IGL</i>	9496	9496	chr8	129301246	<i>PVT1-CCDC26</i>
11/1227	t(11;14)	chr14	105969653	Telomeric	<i>MIR548AS-DAOA-AS1</i>	24389	55470	chr8	128504864	<i>POU5F1B-MYC</i>
12/0213	t(11;14)	chr1	118302879	Telomeric	<i>FAM46C-GDAP2</i>	0	73103	chr8	128866931	<i>MYC-PVT1</i>
12/0365	t(14;16)	chr10	125858805	Telomeric	<i>CHST15-OAT</i>	0	0	chr8	129235977	<i>PVT1-CCDC26</i>
12/0365	t(14;16)	chr17	74521561	Centromeric	<i>RHBDF2-CYGB</i>	30899	645847	chr8	129262577	<i>PVT1-CCDC26</i>
12/0404	t(11;14)	chr11	69425933	Centromeric	<i>MYEOV-CCND1</i>	32171	2368440	chr8	128719531	<i>POU5F1B-MYC</i>

<sup>a</sup>Where > 1 gene is named, the breakpoint is in the intergenic space between genes. <sup>b</sup>Breakpoint within inversion. <sup>c</sup>Confirmed by FISH. <sup>d</sup>Complex rearrangement containing 400 bp of chrX with translocations leading to chromosomes 14 (IGH@) and 8 (PVT1) as well as a t(8;11) and t(11;14). <sup>e</sup>Confirmed by karyotype underlined = derivative does not contain MYC.

Ig loci partner oncogenes is through colocalization of active enhancer elements with the oncogene, we examined the remaining samples with rearrangements for the presence of enhancer elements. We used data from two papers in which binding sites of BRD4 and MED1, which occur at transcriptionally active sites, enhancers and superenhancers in MM1.s cells had been annotated using only enhancer sites on the assembled derivative chromosome.<sup>23,24</sup> As expected, the Ig loci breakpoints were typically close to or within an enhancer/superenhancer (minimum distance=0, maximum distance=26 kb) with the exception of *IGKC* breakpoints, which were ~292 kb from the nearest superenhancer (Table 3). This discrepancy is likely owing to MM1.s cells being a lambda light chain expresser that do not express a kappa light chain. If a cell line expressing a kappa light chain had been used in the analysis an enhancer may have been detected much closer.

In order to determine whether there was an enrichment of superenhancer sites in the vicinity of *MYC* breakpoints, we used the genomic locations of superenhancers from a variety of the cell types determined in Hnisz *et al.*<sup>23</sup> There was a statistically significant enrichment for breakpoints within 1 Mb of a superenhancer in the MM1.s myeloma cell line and in CD19<sup>+</sup> B cells ( $P=0.0049$  and  $0.041$ , respectively). No enrichment was seen with enhancer locations in K562 cells, CD3<sup>+</sup> T cells or

skeletal muscle myoblasts indicating a cell-specific enrichment for superenhancers in the B-cell lineage.

The partner loci to *MYC* are also mostly related to myeloma pathogenesis or B-cell biology (Table 3). In addition to the Ig loci, partner genes of *MYC* rearrangements included *FAM46C*, *KRAS* and *CCND1*. All of these genes are candidates in many genetic studies of myeloma. *FAM46C* is deleted in ~20% of samples and mutated in ~3% of samples.<sup>2,25</sup> *KRAS* is mutated in 31% of samples and *CCND1* is overexpressed in t(11;14) accounting for ~15% of samples.<sup>26,27</sup> In addition, *XBP1* is involved in plasma cell differentiation, the unfolded protein response and is mutated in a low percentage of relapsed refractory myeloma.<sup>26,28</sup> The genes located next to breakpoints in the remaining samples may also be active in B-cell biology or myeloma pathogenesis as recurrent translocations are found near the *CHST15* locus, which is known to be involved in B-cell signaling,<sup>29,30</sup> and *FOXO3*, which is involved in B-cell development.<sup>31</sup> Some rearrangements from these samples are shown in Figure 2 to illustrate the colocalization of superenhancers to *MYC*.

#### Impact on *MYC* expression

Previously published gene expression array data were available on 33 of the samples (Supplementary Table 2).<sup>2</sup> We categorized the

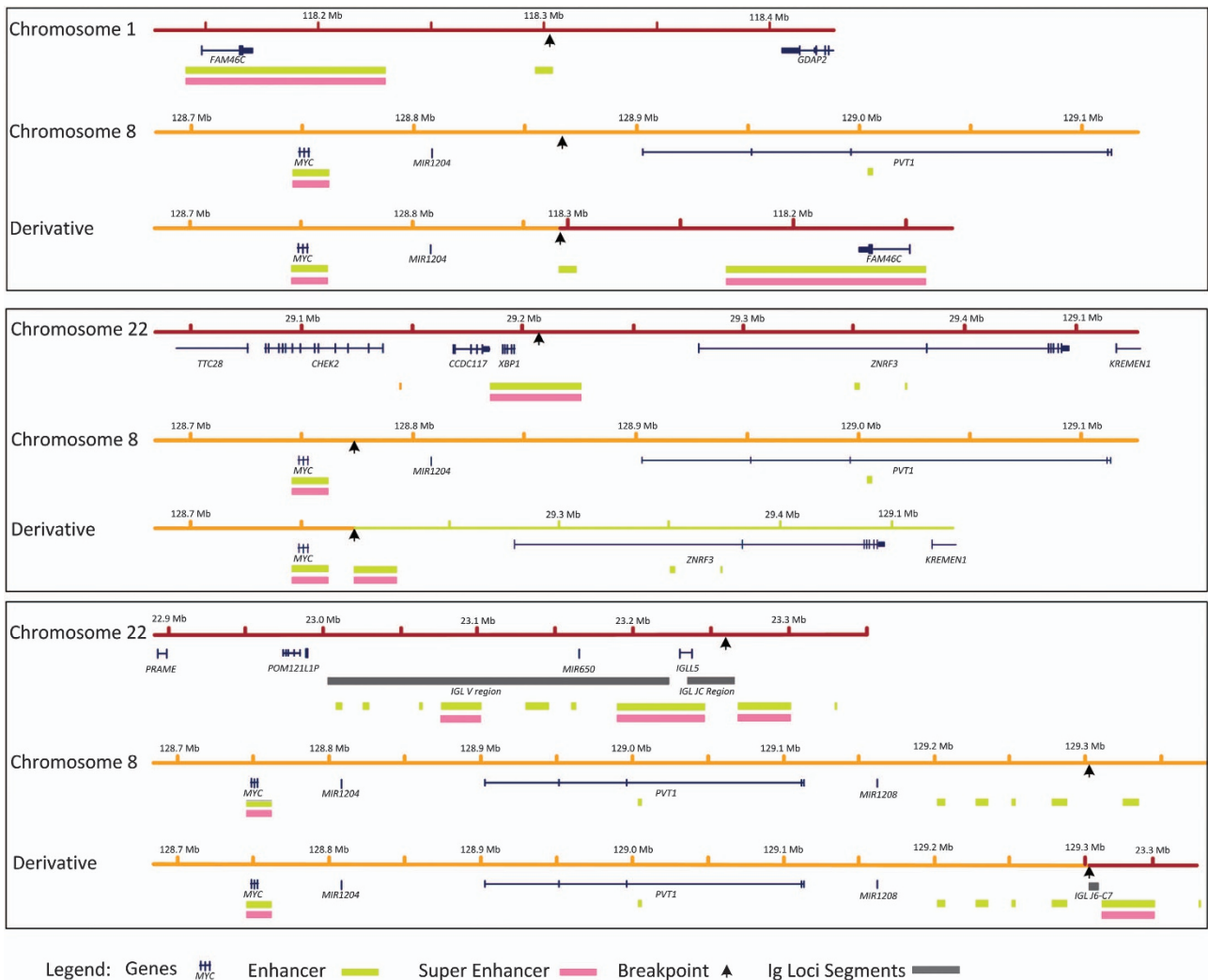


**Figure 2.** *MYC* rearrangements result in superenhancer colocalization on the derivative chromosome. Superenhancer elements are colocalized near to *MYC* from a t(1;8) (top) or a t(8;22) (middle and bottom) where the partner chromosome gene (*FAM46C*, *XBP1* and *IGL*, respectively) has a known function in myeloma or B-cell biology.



samples according to the presence ( $n = 9$ ) or absence ( $n = 24$ ) of a *MYC* translocation, as detected by the capture assay, and used the *MYC* probe set (202431\_s\_at) to examine any difference in expression between the groups. Those samples with any *MYC* translocation had higher expression of *MYC* compared with those without a translocation (median 703.2 vs 2313), but this did not reach significance with this number of samples ( $P = 0.065$ ) (Figure 3a). This was extended in the full Myeloma IX data set for which any translocation was detected by FISH or capture and for which expression array data were available. In this larger data set, samples with any translocation ( $n = 27$ ) had a significantly higher expression of *MYC* (2003 vs 945.8,  $P = 0.009$ ) compared with those with no translocation ( $n = 142$ ), even allowing for those samples on which no capture had been performed (and may contain translocations not detected by FISH) (Figure 3b). The increase in expression of *MYC* is consistent with its deregulation being the central mechanism.

#### Impact on clinical outcome

A subset of patients ( $n = 55$ ) from the capture panel had taken part in the UK MRC Myeloma IX trial, so we performed an analysis of the impact of *MYC* translocations on survival. *MYC* translocations had a significant impact on OS and PFS in univariate analysis (Table 3), which carried over into multivariate analysis, resulting in a significant decrease in OS and PFS for patients with a *MYC* translocation (Figure 4).

#### DISCUSSION

Here, we have investigated the partner loci involved in rearrangements with 8q24, namely *MYC*. We analyzed presenting cases of myeloma characterized by a range of different primary *IGH* translocation events and found evidence of a *MYC* translocation in 21% of samples, making it the most frequent translocation in presenting myeloma cases.

Although FISH analysis of 8q24 rearrangements found no significant association with primary translocation groups, we did find an enrichment for samples with a *MYC* breakpoint in samples that had a t(14;16) and a depletion of samples with a t(4;14) or hyperdiploidy when screened by the sequence capture technique.

Other studies using FISH agree with our FISH-based results in that it has been reported that rearrangements at the *MYC* locus show a similar prevalence in hyperdiploid and non-hyperdiploid tumors<sup>1</sup> or show some trend to being associated with t(4;14).<sup>3</sup> The discrepancy between our capture results and those determined by FISH may lie in the technique used to study the abnormality. One study used both FISH and mapping arrays to examine *MYC* breakpoints and found that 33% of breakpoints detected by array were not detected by routine FISH analysis.<sup>17</sup> Therefore, a higher resolution assay, such as genome sequencing, may identify more breakpoints and explain some of the discrepant results. However, care must be taken regarding the frequency of sequence capture translocations within the primary translocation groups owing to the bias in sample selection and the relatively small number of samples studied.

It is notable that all groups find *MYC* rearrangements to be complex, often involving many chromosomes. We only capture the region surrounding *MYC* and are not able to detect any rearrangements downstream on the partner chromosome, which could result in inversions, insertions or duplications of DNA segments. Whole-genome sequencing of samples will provide more complex and detailed information regarding the final composition of the genome in these samples.

The translocations at 8q24 results in overexpression of *MYC* due to the colocalization of active superenhancers in the partner loci. The obvious examples of this belong to the known active enhancers in the B-cell lineage, the Ig loci, but in addition to these a series of previously unknown partners have also been identified. A similar study in B-cell lymphomas identified non-immunoglobulin partners to *MYC* rearrangements and concluded that these are non-random processes that juxtapose *MYC* with genes involved in lymphomagenesis (namely *BCL6*, *PAX5* and *IKAROS*).<sup>32</sup> We have identified a different set of genes in this study and interestingly these genes are related to B-cell biology and myeloma pathogenesis. We hypothesize that in different diseases with *MYC* rearrangements there is a selection process, which results in active superenhancers from genes that are expressed in that cell type being placed near *MYC*. In all B-cell neoplasias these include the Ig loci, but in different B-cell subtypes the non-Ig loci differ to include those that are expressed in that cell type. In myeloma these non-Ig partner genes include *FAM46C*, *KRAS*, *XBPI*

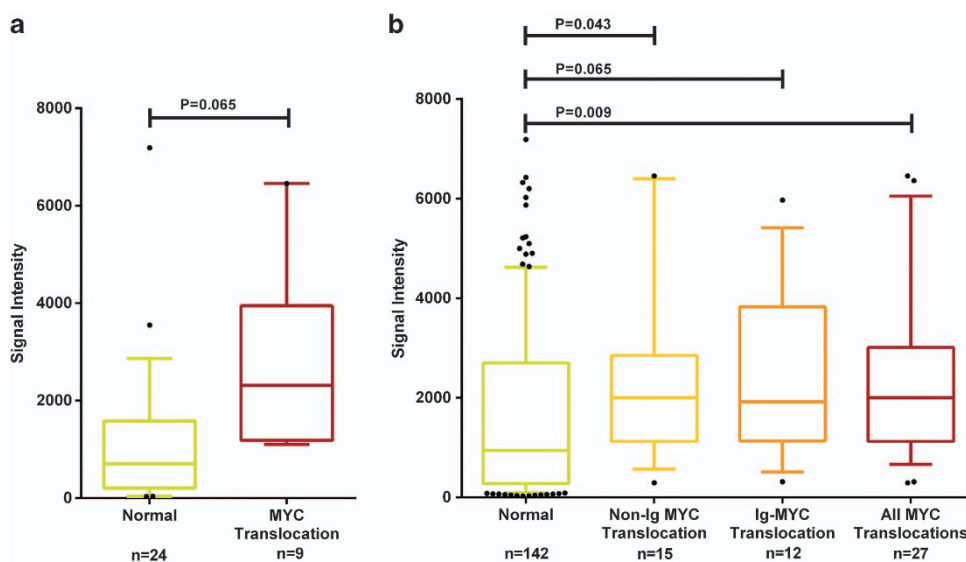


**Figure 3.** Expression of *MYC* in samples with a breakpoint is higher than in those without a breakpoint. (a) Expression data from 33 samples with sequence capture-determined translocations for those samples with no breakpoint at 8q24 (normal) and for those with an identified breakpoint (split *MYC*). (b) Expression data from 169 samples with any translocation detected by capture or FISH. Whisker plots show the 10–90 percentiles.

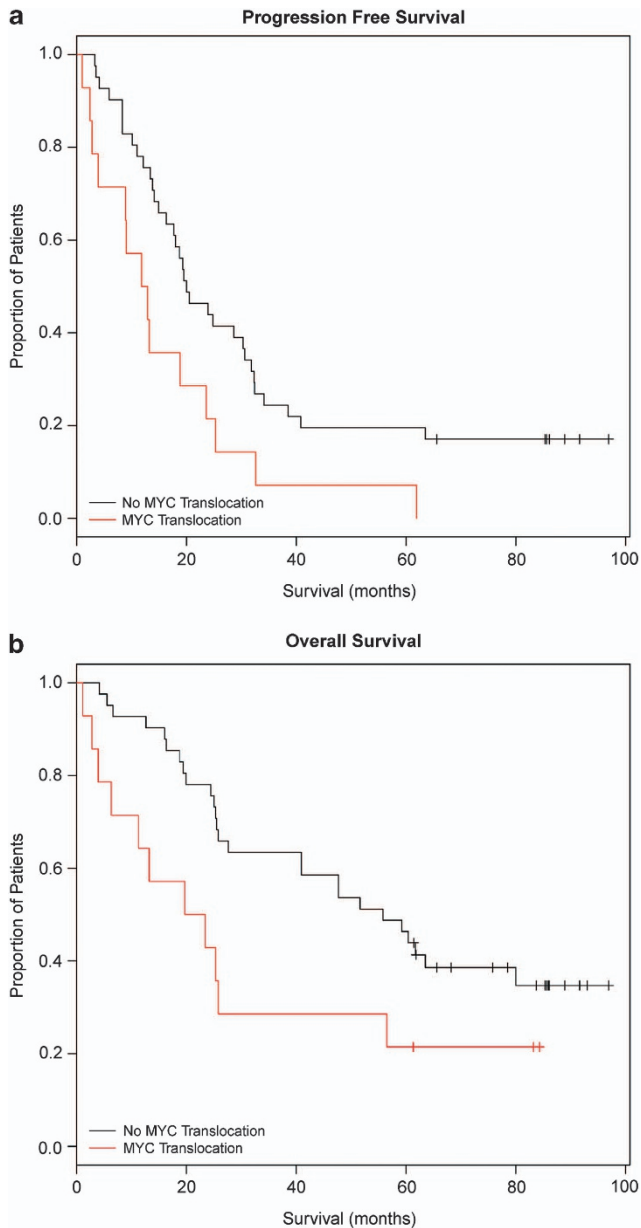


**Figure 4.** Progression-free survival (a) and Overall-free survival (b) in patients with a MYC breakpoint is significantly decreased compared with those without a breakpoint. PFS  $P=0.032$ , OS  $P=0.035$ . Data adjusted for confounding variables in Tables 4a, b and c.

and *CCND1*. The other partner genes identified here, which have no known function in myeloma or plasma cells, are likely also to be important in plasma cell development or myeloma disease as they have active superenhancers that are sequestered by MYC.

Some of the loci identified have active superenhancers up to 22 Mb away from the breakpoint. These distal superenhancers may be responsible for MYC overexpression, but as these results are based solely on data from the MM1.s cell line<sup>24</sup> it may be that in different myeloma cell types an enhancer closer to the breakpoint is active, and it is this as yet unidentified superenhancer that is located near MYC in this patient. This argument is exemplified by the lack of a superenhancer at the *IGK* locus in MM1.s and can be explained as this cell line expresses the lambda light chain and not the kappa light chain.<sup>33</sup> Similar studies involving a large cohort of myeloma cell lines would give further insight into the complex nature of superenhancers in this disease.

**Table 4a.** Clinical characteristics of MYC-translocated samples

Variable	Number of patients	PFS		OS	
		Months	P-value	Months	P-value
MYC translocation	14	11.8	0.016	19.7	0.043
No MYC translocation	41	20.0		55.8	
t(14;16)	9	9.0	0.006	11.2	0.095
No t(14;16)	46	20.0		47.7	
Adverse <i>IGH</i> translocation	27	13.4	0.018	25.5	0.021
No adverse <i>IGH</i> translocation	28	24.8		61.7	
ISS 1	7	61.9	0.013	NR	0.018
ISS 2	15	23.9		60.4	
ISS 3	16	13.8		27.6	
Eligible for intensive pathway <sup>a</sup>	36	25.3	<0.001	80.0	<0.001
Not eligible for intensive pathway <sup>a</sup>	19	11.8		23.4	

Abbreviations: OS, overall survival; PFS, progression-free survival. Univariate analysis—statistically significant. <sup>a</sup>Patients treated according to the intensive pathway received autologous stem cell transplantation, whereas patients not eligible entered the non-intensive pathway and were treated only with attenuated doses of chemotherapy.

**Table 4b.** Multivariate analysis of variables significantly associated with an improved PFS

Variable	P-value	Hazard ratio	95% CI
Absence of adverse translocation	0.03	2.763	1.105–6.908
Absence of MYC translocation	0.035	3.094	1.081–8.856
Treatment on the intensive path	<0.001	5.871	2.186–15.766

Abbreviations: CI, confidence interval; PFS, progression-free survival.

**Table 4c.** Multivariate analysis of variables significantly associated with an improved OS

Variable	P-value	Hazard ratio	95% CI
Absence of adverse translocation	0.010	4.861	1.450–16.293
Absence of MYC translocation	0.032	4.077	1.125–14.785
Treatment on the intensive path	0.001	6.528	2.196–19.404

Abbreviations: CI, confidence interval; OS, overall survival.

As the mechanism of action for MYC overexpression is through the juxtaposition of superenhancers specific to each disease, it is possible that this unifying mechanism can be therapeutically targeted. Given that it has been shown that superenhancers can be disrupted using BET-bromodomain inhibitors, such as JQ1,<sup>24</sup> it makes patients with MYC rearrangements good candidates for treatment with this class of drugs. We show here that patients identified with a MYC translocation have a poor PFS and OS compared with those with no rearrangement. If these patients could be identified in advance they may benefit from treatment with this class of targeted drugs.

#### ACKNOWLEDGEMENTS

We acknowledge The Institute of Cancer Research Tumour Profiling Unit for their support and technical expertise in this study. This work was supported by a Myeloma UK program grant, a CRUK CTAAC sample collection grant and funds from the National Institute of Health Biomedical Research Centre at the Royal Marsden Hospital. FED is a Cancer Research UK Senior Clinical Fellow.

## REFERENCES

- Gabrea A, Martelli ML, Qi Y, Roschke A, Barlogie B, Shaughnessy JD Jr *et al*. Secondary genomic rearrangements involving immunoglobulin or MYC loci show similar prevalences in hyperdiploid and nonhyperdiploid myeloma tumors. *Genes Chromosomes Cancer* 2008; **47**: 573–590.
- Walker BA, Leone PE, Chiecchio L, Dickens NJ, Jenner MW, Boyd KD *et al*. A compendium of myeloma-associated chromosomal copy number abnormalities and their prognostic value. *Blood* 2010; **116**: e56–e65.
- Avet-Loiseau H, Gerson F, Magrangeas F, Minvielle S, Harousseau JL, Bataille R *et al*. Rearrangements of the c-myc oncogene are present in 15% of primary human multiple myeloma tumors. *Blood* 2001; **98**: 3082–3086.
- Dang CV. MYC on the path to cancer. *Cell* 2012; **149**: 22–35.
- Chesi M, Robbiani DF, Sebag M, Chng WJ, Affer M, Tiedemann R *et al*. AID-dependent activation of a MYC transgene induces multiple myeloma in a conditional mouse model of post-germinal center malignancies. *Cancer Cell* 2008; **13**: 167–180.
- Chng WJ, Huang GF, Chung TH, Ng SB, Gonzalez-Paz N, Troska-Price T *et al*. Clinical and biological implications of MYC activation: a common difference between MGUS and newly diagnosed multiple myeloma. *Leukemia* 2011; **25**: 1026–1035.
- Holien T, Vatsveen TK, Hella H, Waaga A, Sundan A. Addiction to c-MYC in multiple myeloma. *Blood* 2012; **120**: 2450–2453.
- Dib A, Gabrea A, Glebov OK, Bergsagel PL, Kuehl WM. Characterization of MYC translocations in multiple myeloma cell lines. *J Natl Cancer Inst Monogr* 2008; **39**: 25–31.
- Sawyer JR, Lukacs JL, Thomas EL, Swanson CM, Goosen LS, Sammartino G *et al*. Multicolour spectral karyotyping identifies new translocations and a recurring pathway for chromosome loss in multiple myeloma. *Br J Haematol* 2001; **112**: 167–174.
- Avet-Loiseau H, Daviet A, Brigaudeau C, Callet-Bauchu E, Terre C, Lafage-Pochitaloff M *et al*. Cytogenetic, interphase, and multicolor fluorescence *in situ* hybridization analyses in primary plasma cell leukemia: a study of 40 patients at diagnosis, on behalf of the Intergroupe Francophone du Myelome and the Groupe Francais de Cytogenetique Hematologique. *Blood* 2001; **97**: 822–825.
- Mohamed AN, Bentley G, Bonnett ML, Zonder J, Al-Katib A. Chromosome aberrations in a series of 120 multiple myeloma cases with abnormal karyotypes. *Am J Hematol* 2007; **82**: 1080–1087.
- Fabris S, Storlazzi CT, Baldini L, Nobili L, Lombardi L, Maiolo AT *et al*. Heterogeneous pattern of chromosomal breakpoints involving the MYC locus in multiple myeloma. *Genes Chromosomes Cancer* 2003; **37**: 261–269.
- Nagoshi H, Taki T, Hanamura I, Nitta M, Otsuki T, Nishida K *et al*. Frequent PVT1 rearrangement and novel chimeric genes PVT1-NBEA and PVT1-WWOX occur in multiple myeloma with 8q24 abnormality. *Cancer Res* 2012; **72**: 4954–4962.
- Zeidler R, Joos S, Delecluse HJ, Klobeck G, Vuillaume M, Lenoir GM *et al*. Breakpoints of Burkitt's lymphoma t(8;22) translocations map within a distance of 300 kb downstream of MYC. *Genes Chromosomes Cancer* 1994; **9**: 282–287.
- Ross FM, Ibrahim AH, Vilain-Holmes A, Winfield MO, Chiecchio L, Protheroe RK *et al*. Age has a profound effect on the incidence and significance of chromosome abnormalities in myeloma. *Leukemia* 2005; **19**: 1634–1642.
- Chiecchio L, Protheroe RK, Ibrahim AH, Cheung KL, Rudduck C, Dagrada GP *et al*. Deletion of chromosome 13 detected by conventional cytogenetics is a critical prognostic factor in myeloma. *Leukemia* 2006; **20**: 1610–1617.
- Chiecchio L, Dagrada GP, White HE, Townsend MR, Protheroe RK, Cheung KL *et al*. Frequent upregulation of MYC in plasma cell leukemia. *Genes Chromosomes Cancer* 2009; **48**: 624–636.
- Walker BA, Wardell CP, Johnson DC, Kaiser MF, Begum DB, Dahir NB *et al*. Characterization of IGH locus breakpoints in multiple myeloma indicates a subset of translocations appear to occur in pregerminal center B cells. *Blood* 2013; **121**: 3413–3419.
- Rausch T, Zichner T, Schlattl A, Stutz AM, Benes V, Korbel JO. DELLY: structural variant discovery by integrated paired-end and split-read analysis. *Bioinformatics* 2012; **28**: i333–i339.
- Goecks J, Nekrutenko A, Taylor J, Galaxy T. Galaxy: a comprehensive approach for supporting accessible, reproducible, and transparent computational research in the life sciences. *Genome Biol* 2010; **11**: 8.
- Chiecchio L, Dagrada GP, Ibrahim AH, Dachs Cabanas E, Protheroe RK, Stockley DM *et al*. Timing of acquisition of deletion 13 in plasma cell dyscrasias is dependent on genetic context. *Haematologica* 2009; **94**: 1708–1713.
- Kaiser MF, Walker BA, Hockley SL, Begum DB, Wardell CP, Gonzalez D *et al*. A TC classification-based predictor for multiple myeloma using multiplexed real-time quantitative PCR. *Leukemia* 2013; **27**: 1754–1757.
- Hnisz D, Abraham B, Lee T, Lau A, Saint-André V, Sigova A *et al*. Super-enhancers in the control of cell identity and disease. *Cell* 2013; **155**: 934–947.
- Loven J, Hoke HA, Lin CY, Lau A, Orlando DA, Vakoc CR *et al*. Selective inhibition of tumor oncogenes by disruption of super-enhancers. *Cell* 2013; **153**: 320–334.
- Boyd KD, Ross FM, Walker BA, Wardell CP, Tapper WJ, Chiecchio L *et al*. Mapping of chromosome 1p deletions in myeloma identifies FAM46C at 1p12 and CDKN2C at 1p32.3 as being genes in regions associated with adverse survival. *Clin Cancer Res* 2011; **17**: 7776–7784.
- Chapman MA, Lawrence MS, Keats JJ, Cibulskis K, Sougnez C, Schinzel AC *et al*. Initial genome sequencing and analysis of multiple myeloma. *Nature* 2011; **471**: 467–472.
- Walker BA, Wardell CP, Melchor L, Hulkki S, Potter NE, Johnson DC *et al*. Intracлонаl heterogeneity and distinct molecular mechanisms characterize the development of t(4;14) and t(11;14) myeloma. *Blood* 2012; **120**: 1077–1086.
- Morgan GJ, Walker BA, Davies FE. The genetic architecture of multiple myeloma. *Nat Rev Cancer* 2012; **12**: 335–348.
- Verkoczy L, Guinn B, Berinstein N. Characterization of the human B cell RAG-associated gene, hBRAG, as a B cell receptor signal-enhancing glycoprotein dimer that associates with phosphorylated proteins in resting B cells. *J Biol Chem* 2000; **275**: 20967–20979.
- Verkoczy L, Marsden P, Berinstein N. hBRAG a novel B cell lineage cDNA encoding a type II transmembrane glycoprotein potentially involved in the regulation of recombination activating gene 1 (RAG1). *Eur J Immunol* 1998; **28**: 2839–2853.
- Hinman R, Nichols W, Diaz T, Gallardo T, Castrillon D, Satterthwaite A. Foxo3<sup>-/-</sup> mice demonstrate reduced numbers of pre-B and recirculating B cells but normal splenic B cell sub-population distribution. *Int Immunol* 2009; **21**: 831–842.
- Bertrand P, Bastard C, Maingonnat C, Jardin F, Maisonneuve C, Courel MN *et al*. Mapping of MYC breakpoints in 8q24 rearrangements involving non-immunoglobulin partners in B-cell lymphomas. *Leukemia* 2007; **21**: 515–523.
- Moalli PA, Pillay S, Weiner D, Leikin R, Rosen ST. A mechanism of resistance to glucocorticoids in multiple myeloma: transient expression of a truncated glucocorticoid receptor mRNA. *Blood* 1992; **79**: 213–222.



This work is licensed under a Creative Commons Attribution-NonCommercial-NoDerivs 3.0 Unported License. To view a copy of this license, visit <http://creativecommons.org/licenses/by-nc-nd/3.0/>

Supplementary Information accompanies this paper on Blood Cancer Journal website (<http://www.nature.com/bcj>)